Modeling endocrine control of the pituitary-ovarian axis: Androgenic influence and chaotic dynamics *

Angelean O. Hendrix

Department of Mathematics

North Carolina State University

Raleigh, NC †‡

Claude L. Hughes

Cardiovascular and Metabolic Unit, Quintiles, Inc.

Department of Mathematics, North Carolina State University

Department of Obstetrics and Gynecology, Duke University Medical Center

Durham, NC

James F. Selgrade

Department of Mathematics and Biomathematics Program

North Carolina State University

Raleigh, NC

*Support by NSF grants DMS-0920927 and DMS-1225607

†This material is based upon work supported by the National Science Foundation Graduate Research Fellowship under Grant No. DGE-0750733

‡Corresponding Author Email: aohendri@ncsu.edu

Abstract

Mathematical models of the hypothalamus-pituitary-ovarian axis in women were first developed by Schlosser and Selgrade in 1999, with subsequent models of Harris-Clark *et al.* (2003) and Pasteur and Selgrade (2011). These models produce periodic in-silico representation of luteinizing hormone (LH), follicle stimulating hormone (FSH), estradiol (E2), progesterone (P4), inhibin A (InhA), and inhibin B (InhB). Polycystic ovarian syndrome (PCOS), a leading cause of cycle irregularities, is seen as primarily a hyper-androgenic disorder. Therefore, including androgens into the model is necessary to produce simulations relevant to women with PCOS. Because testosterone (T) is the dominant female androgen, we focus our efforts on modeling pituitary feedback and inter-ovarian follicular growth properties as functions of circulating total T levels. Optimized parameters simultaneously simulate LH, FSH, E2, P4, InhA, and InhB levels of Welt *et al.* (1999) and total T levels of Sinha-Hikim *et al.* (1998). The resulting model is a system of 16 ordinary differential equations, with at least one stable periodic solution. Maciel *et al.* (2004) hypothesized that retarded early follicle growth resulting in "stockpiling" of preantral follicles contributes to PCOS etiology. We present our investigations of this hypothesis and show that varying a follicular growth parameter produces preantral stockpiling and a period-doubling cascade resulting in apparent chaotic menstrual cycle behavior. The new model may allow investigators to study possible interventions returning acyclic patients to regular cycles and guide developments of individualized treatments for PCOS patients.

1 Introduction

Periodic fluctuations in pituitary and ovarian hormones regulate the human female reproductive cycle. Gonadotropin-releasing hormone (GnRH) from the hypothalamus prompts the pituitary to produce follicle stimulating hormone (FSH) and luteinizing hormone (LH) which control ovarian follicular development and sex hormone secretion (Yen [51], Hotchkiss and Knobil [16]). The ovaries secrete estradiol (E2), progesterone (P4), inhibin A (InhA), inhibin B (InhB) and androgens which in turn affect the synthesis and release of FSH and LH (Karsch *et al.* [19], Liu and Yen [23]) via positive and negative feedback relationships. Models for hormonal regulation of the menstrual cycle have been constructed using systems of ordinary differential equations where state variables represent serum hormone levels or different stages of monthly ovarian development, e.g., Harris-Clark *et al.*, 2003 [14], Reinecke and Deuflhard, 2007 [38], and Pasteur and Selgrade, 2011 [35]. The model presented here expands on the models of Harris-Clark *et al.* [14] and Pasteur and Selgrade [35] by including the effects of the androgen testosterone (T) on the brain and on the ovaries.

Pulses of gonadotropin-releasing hormone (GnRH) produced by the hypothalamus on a time scale of minutes and hours cause pulses of FSH and LH to be produced by the pituitary. Because the ovaries respond to average daily blood levels (Odell [31]), our models track average daily concentrations of FSH and LH. Hence we lump the effects of the hypothalamus and the pituitary together and just consider the synthesis and release of FSH and LH on the time scale of days. This simplification results in models which give good fit to the daily serum data of McLachlan *et al.*, 1990 [28], and to the data of Welt *et al.*,1999 [49], and which avoid the complication of multiple time scales. These models exhibit novel features, e.g., two stable periodic solutions — one ovulatory and the other non-ovulatory (Harris-Clark *et al.* [14]). The non-ovulatory cycle lacks a surge in LH and has a contraceptive level of E2. Model simulations illustrate how exogenous P4 may be used to perturb the

non-ovulatory cycle to the ovulatory cycle and how exogenous E2 may be used to perturb the ovulatory cycle to the non-ovulatory cycle (see [14]). The latter is an example of how environmental estrogens may disrupt a woman's menstrual cycle. In addition, Selgrade [43] and Margolskee and Selgrade [26] explain the bistable behavior by analyzing bifurcation diagrams with respect to a parameter which measures the LH response of the pituitary to E2 priming. The review article by Vetharaniam *et al.*, 2010 [48], describes many models of hormonal control of the female reproductive cycle and discusses their strengths and limitations.

The development of the follicle which releases its ovum in a specific menstrual cycle begins at least 60 days before that cycle (Nussey and Whitehead [30]). To model hormonal regulation of these early growing follicles, preantral and early antral stages must be included. Abnormal development during this period of early growth may result in cycle irregularities such as polycystic ovarian syndrome (PCOS), a leading cause of female infertility [1, 3, 11, 51]. In fact, Maciel *et al.* [25] reported a "stockpiling" of preantral follicles in women with PCOS as compared to normally cycling women. The development of preantral follicles is gonadotropin independent but intra-ovarian factors (Skinner [46], Reddy *et al.* [37], Maciel *et al.* [25]) influence the early growth and the transition to the antral stage. Also, androgen receptors appear before FSH receptors (Rice *et al.* [39]), so in this study we consider the effects of testosterone (T) on preantral and early antral follicles. Understanding how variations in hormone levels and key ovarian growth parameters alter early follicular development may predict disordered ovulation three months later.

To this end, we describe a mathematical model for menstrual cycle regulation which includes 12 distinct stages of ovarian development and 7 pituitary and ovarian hormones. Our model builds on previous models (e.g., see [14,17,34,42,44]) for endocrine control of the cycle but adds three new stages of follicular development and includes the effects of T on the ovaries and on the pituitary. First, we discuss the biological background and the model

equations. Second, parameters are identified using the data of Welt *et al.* [49] and Sinha-Hikim *et al.* [45]. Third, model simulations are presented and compared to data. Finally, we illustrate how decreasing the transfer parameter between the preantral and early antral follicular stages results in the stockpiling of preantral follicles and a significant alteration in hormone levels. In fact, by varying this parameter we demonstrate a period-doubling cascade of bifurcations that results in chaotic hormone fluctuations.

2 Biological Background and Model Development

2.1 Follicular Growth and Ovarian Stages

The normal adult menstrual cycle is approximately 28 days in duration and can be divided into two phases: follicular (menstruation to ovulation) and luteal (ovulation to menstruation). A cohort of primordial follicles is activated at least 60 days before the LH surge promotes ovulation of the dominant follicle from that particular cohort [12]. Upon activation, this cohort migrates to the medullary region of the ovary, returning to the surface of the ovary in a process known as "emergence" as maturation proceeds [10]. During this time follicles are classified into at least 4 categories: preantral, early antral, antral and recruited. The preantral stage accounts for the majority of the gonadotropin independent follicular growth. Thereafter follicles begin to develop an antrum and sensitivity to FSH increases rapidly [12]. A significant portion of these antral follicles degenerate through atresia while larger follicles with additional FSH receptors enter a recruitment phase. This development establishes the beginning the follicular phase of the monthly cycle. During this fourteen day period, evidence suggests FSH must rise above a threshold level for five days during which a select subgroup of follicles experiences rapid growth. This span of time in the menstrual cycle is referred to as the FSH window [9]. The dominant follicle (the one destined for

ovulation) is selected from this cohort by its acquisition of LH receptors. As serum FSH begins to decline, non-dominant follicles begin to degenerate. The dominant follicle reaches a diameter of about 20 mm just prior to mid cycle and secretes large amounts of E2 which promotes pituitary LH production. Once LH reaches surge levels, the dominant follicle releases its ovum and is transformed into the corpus luteum (CL). CL tissue develops a yellow appearance, increases in mass until day nineteen of the cycle and produces high levels of E2, P4 and InhA. Ovarian steroid production peaks at day twenty-one and, in the absence of pregnancy, declines with the regression of the CL during the remainder of the luteal phase of the menstrual cycle.

2.2 Intra-Ovarian Growth Regulation

Histological samples of ovarian tissue can reveal diverse numbers of follicles from 1 mm to 20 mm in diameter during most of the menstrual cycle [12]. As current ultrasound technology is best at identifying follicles greater than 2 mm [18], it is common to consider this as the point of primary follicle activation. A slight elevation in ovarian mass can be observed with the appearance of the dominant follicle [22] with the peak in ovarian mass occurring at approximately day 19 of the cycle [22] due to CL development. These findings suggest the existence of a signaling mechanism that maintains the total mass near steady state. Local factors identified in follicular fluid analysis are commonly accepted as major contributors in this regulation. It is hypothesized that follicles in a more advanced growth stage regulate activation of a new wave of follicles through the use of insulin like growth factors [24], transforming growth factor ($TGF\beta 1$) [21], granulosa-theca cell factors [32], antimüllerian hormone [11], and androgens [39]. Follicular fluid concentrations of growth factors are significant and change dynamically, but it seems implausible that corresponding changes in serum levels will be detectable. We therefore focus our efforts on serum levels

of T with the knowledge that androgen receptors have been found in granulosa cells of developing follicles as small as 0.2 mm, before FSH receptors appear [39]. This allows us to capture fluctuations in follicular growth rates by integrating T levels into a subsystem of ovarian follicular development that self-regulates its total mass.

2.3 Ovarian Modeling Technique

In our attempt to model the ovarian mass of preantral and small antral follicles we utilize mathematical theories of mass action kinetics. Often used to describe chemical reactions where the total mass or volume of a system remains constant while the individual components change dynamically, the mass action approach allows us to reflect total mass steady state regulation. The model equations are built to reflect an interdependent shift of mass through three stages of follicular maturity, represented by the state variables $PrA1$ (preantral follicle 1), $PrA2$ (preantral follicle 2) and $SmAn$ (small antral follicle). This approach captures the intra-ovarian effects on early follicular development reviewed in section 2.2. Transitions through these stages depend on the masses of adjacent stages and available hormone levels (see Figure 1). We assume that proximity between follicles determines the magnitude of interfollicular signaling with the most significant effects coming from the subsequent maturity levels as the follicles migrate towards the outer cortex of the ovary. This allows us to emulate intra-ovarian signaling when follicular fluid levels of growth factors cannot be quantified. Differential equations are then mechanistically constructed for each of our state variables.

The growth term in our first stage, $PrA1$, has a constant rate, m_1, of primordial follicle recruitment as suggested by Gougeon [12]. We introduce a T dependent transfer term that scales the product of the current mass of preantral follicles ($PrA1$) with the mass of the next stage of maturity ($PrA2$). This term reflects the appearance of androgen receptors

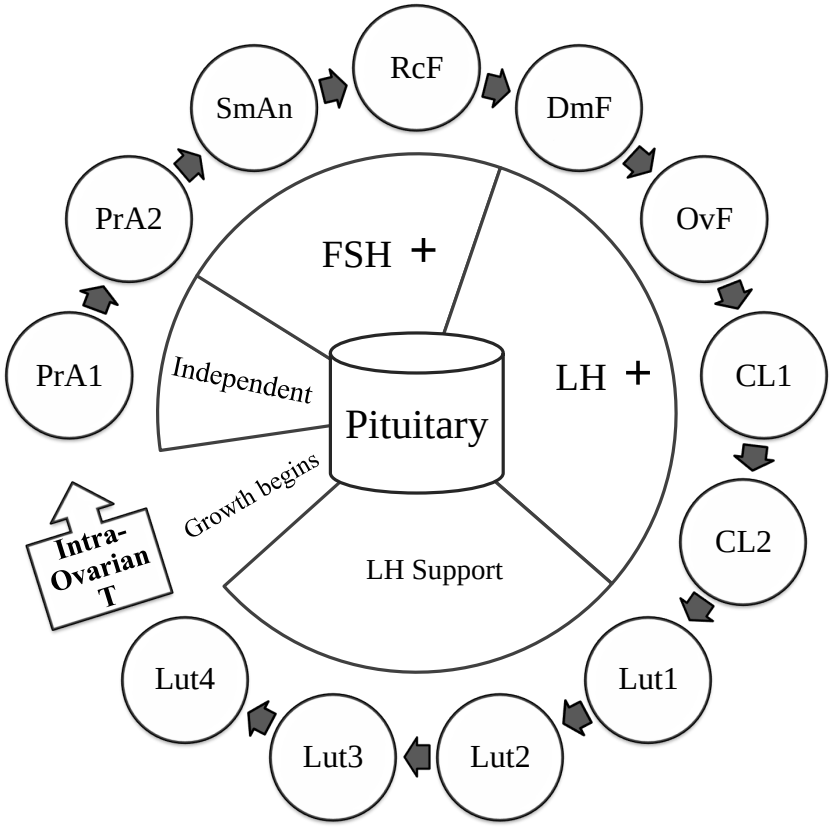

Figure 1: State variables representing 12 stages of follicular development are shown. Follicle growth begins with the $PrA1$ stage and continues in a clockwise direction for a complete cycle. The pie chart indicates the timing of the regulatory effects of luteinizing hormone (LH) and follicle stimulating hormone (FSH) on follicular development.

before gonadotropin growth begins and contains an exponential, η, introduced to increase the rate of stimulatory response to T [39]. The equation for $PrA1$ becomes:

$$\frac{d}{dt}PrA1 = m_1 - m_2 \cdot T^{\eta} \cdot PrA1 \cdot PrA2 \tag{1}$$

The product $PrA1 \cdot PrA2$ quantifies the intra-ovarian growth factors and becomes the growth term for $PrA2$. We then shift our mass from $PrA2$ utilizing an FSH dependent

threshold term (e.g., see Zeleznik [52])

$$m_3 \cdot \frac{FSH^{\nu}}{Km_{FSH}^{\nu} + FSH^{\nu}} \cdot$$

This gradual acquisition of receptors and saturation behavior is translated mathematically through a Hill function whose product with the current stage, $PrA2$, and following stage, $SmAn$, defines our next transfer term.

$$\frac{d}{dt}PrA2 = m_2 \cdot T^{\eta} \cdot PrA1 \cdot PrA2 - m_3 \cdot \frac{FSH^{\nu}}{Km_{FSH}^{\nu} + FSH^{\nu}} \cdot PrA2 \cdot SmAn \qquad (2)$$

As the mass of $PrA2$ is dependent on that of $SmAn$, there exists an indirect effect of $SmAn$ on our first stage, $PrA1$. This assumes that migration increases the distance from $SmAn$ follicles to the $PrA1$ follicles and, therefore, the interfollicular signaling between the two decreases. The last stage of mass action dependence, $SmAn$, provides the small antral follicle mass available for recruitment whose growth is partially regulated by follicles in $PrA2$, and indirectly by follicles in $PrA1$ through its inclusion in the equation for $PrA2$.

$$\frac{d}{dt}SmAn = m_3 \cdot \frac{FSH^{\nu}}{Km_{FSH}^{\nu} + FSH^{\nu}} \cdot PrA2 \cdot SmAn - b \cdot FSH^{\varrho} \cdot SmAn \cdot RcF \qquad (3)$$

For the decay term we assume that the rate of FSH receptor acquisition rapidly increases to a point directly proportional to the natural rise in follicular phase FSH at the beginning

of the follicular phase [12], rather than a threshold response used in the previous stage. Similarly, the transfer of mass from $SmAn$ is affected by the existing mass in the subsequent stage RcF whose growth is affected by $SmAn$ directly (see eq. 4) and by $PrA1$ and $PrA2$ indirectly (see eqs. 2, 3).

To reflect the increasing ovarian mass during the follicular and luteal phases of the cycle, linear growth and decay terms are employed in 9 different stages which represent ovarian development during the monthly cycle (Figure 1). RcF represents recruited follicles with additional growth stimulated by FSH and transfer dependent on the appearance of LH receptors. Our equation for RcF marks transition from the mass action terms to linear compartmental terms as in Harris-Clark *et al.* [14]. These compartmental terms permit total ovarian mass to increase as the ovaries approach the time at which a dominant follicle is selected. DmF and OvF represent the dominant and ovulatory follicle. $CL1$ and $CL2$ portray the transition to the corpus luteum. The luteal phase consists of the four stages $Luti$, $i = 1, \ldots, 4$ representing the regression of the CL and conclusion of the current monthly cycle (Figure 1). These 9 stages correspond to the ovarian model of Harris-Clark *et al.* [14]. The growth and decay of these stages are influenced by the gonadotropins as indicated in the following differential equations:

$$\frac{d}{dt}RcF = b \cdot FSH^{\varrho} \cdot SmAn \cdot RcF + (c_1 \cdot FSH - c_2 \cdot LH^{\alpha}) \cdot RcF \tag{4}$$

$$\frac{d}{dt}DmF = c_2 \cdot LH^{\alpha} \cdot RcF + (c_3 \cdot LH^{\beta} - c_4 \cdot LH^{\xi}) \cdot DmF \tag{5}$$

$$\frac{d}{dt}OvF = c_4 \cdot LH^{\xi} \cdot DmF - c_5 \cdot LH^{\gamma} \cdot OvF \tag{6}$$

$$\frac{d}{dt}CL1 = c_5 \cdot LH^{\gamma} \cdot OvF - d_1 \cdot CL1 \tag{7}$$

$$\frac{d}{dt}CL2 = d_1 \cdot CL1 - d_2 \cdot CL2 \tag{8}$$

$$\frac{d}{dt}Lut1 = d_2 \cdot CL2 - k_1 \cdot Lut1 \tag{9}$$

$$\frac{d}{dt}Lut2 = k_1 \cdot Lut1 - k_2 \cdot Lut2 \tag{10}$$

$$\frac{d}{dt}Lut3 = k_2 \cdot Lut2 - k_3 \cdot Lut3 \tag{11}$$

$$\frac{d}{dt}Lut4 = k_3 \cdot Lut3 - k_4 \cdot Lut4 \tag{12}$$

Clearance from the blood for the ovarian hormones is on a fast time scale (Baird *et al.* [6]) as compared to ovarian development and clearance for the pituitary hormones. Hence, we assume that circulating levels of the ovarian hormones are maintained at a quasi-steady state (Keener and Sneyd [20]) as did Bogumil *et al.* [7]. Implementation of this approach results in using linear combinations of the 12 ovarian stages to obtain serum levels of $E2$, $P4$, $InhA$, $InhB$ and T. The following five auxiliary equations result:

Auxiliary Equations (A)

$$E2 = e_0 + e_1 \cdot DmF + e_2 \cdot Lut4 \tag{A1}$$

$$P4 = p_1 \cdot Lut3 + p_2 \cdot Lut4 \tag{A2}$$

$$InhA = h_0 + h_1 \cdot OvF + h_2 \cdot Lut2 + h_3 \cdot Lut3 \tag{A3}$$

$$InhB = j_1 + j_2 \cdot PrA2 + j_3 \cdot SmAn + j_4 \cdot RcF + j_5 \cdot CL1^{j_6} \tag{A4}$$

$$T = t_1 + t_2 \cdot PrA2 + t_3 \cdot SmAn + t_4 \cdot RcF + t_5 \cdot DmF + t_6 \cdot OvF + t_7 \cdot Lut1 + t_8 \cdot Lut3 \tag{A5}$$

The equation for circulating T was originally constructed to be a linear combination of ovarian stages (1-12). However, we assume that hormones are not produced by newly

activated follicles in $PrA1$ and parameter fitting to data revealed little to no synthesis of T from the ovarian stages $CL1$, $CL2$, $Lut2$, and $Lut4$.

2.4 Androgenic Feedback on the Pituitary

Recent studies of T feedback suggest that it is an important component in the modulation of LH secretion by the pituitary in women. In human females elevated T is significantly correlated with elevated basal LH and dampened LH surge [9, 47]. Animal models have shown that T is a necessary component in priming the pituitary for GnRH induced LH synthesis, e.g., see Pielecka *et al.* [36] and Yasin *et al.* [50]. Ovariectomized rats subjected to exogenous GnRH pulses showed significantly greater LHβ mRNA response when pretreated with T implants versus controls (Yasin *et al.* [50]). Treatment levels, similar to those documented at proestrous, demonstrate a 3-fold increase in the LHβ mRNA response to GnRH when compared to untreated controls. Yasin *et al.* [50] noted that their results were independent of aromatization of T to estradiol. Hence, we suggest that T may directly stimulate LH synthesis and will include such an effect in our model.

2.5 Hypothalumus-Pituitary Modeling Technique

Schlosser and Selgrade 2000 [42] proposed a pair of differential equations for each gonadotropin to model the hypothalamically controlled pituitary response to ovarian hormones. These equations described the synthesis in the pituitary, the release into the blood and clearance from the blood of LH and FSH, see Figure 2. The coupling of hypothalamic and pituitary actions allowed the system to predict serum levels of gonadotropins on a daily time scale consistent with published clinical data (McLachlan *et al.* [28] and Welt *et al.* [49]). In these differential equations, the state variables RP_{LH} and RP_{FSH} represent the amounts of gonadotropins synthesized in the pituitary via GnRH signalling and the state

variables LH and FSH represent blood concentrations. The original model of Schlosser and Selgrade [42] assumed a baseline LH synthesis rate v_0 independent of E2. Motivated by Yasin *et al.* [50], for our model we assume that this baseline rate depends on T, see eq. (13).

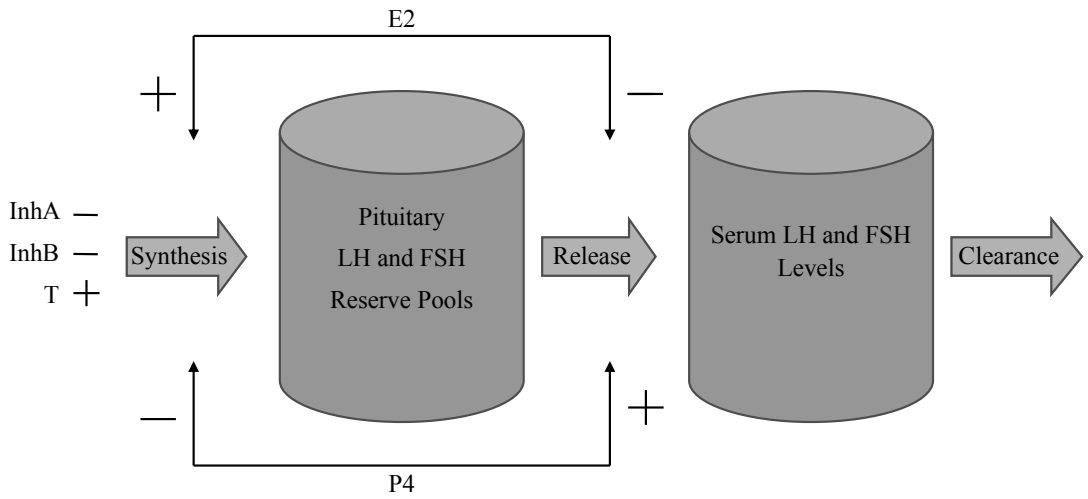

Figure 2: Ovarian control of the GnRH modulated pituitary synthesis and release of LH and FSH. Stimulatory and inhibitory effects are denoted by + and - signs, respectively.

$$\frac{d}{dt}RP_{LH} = \frac{v_0 \cdot T(t-d_T)^{\kappa} + v_1 \cdot \dfrac{E2(t-d_E)^a}{(Km_{LH}^a + E2(t-d_E)^a)}}{\left(1 + \dfrac{P4(t-d_P)}{Ki_{LH}}\right)} - k_{LH} \cdot \frac{\left(1 + c_{LHp} \cdot P4^{\delta}\right)}{(1 + c_{LHe} \cdot E2)} \cdot LH \tag{13}$$

$$\frac{d}{dt}LH = \frac{1}{v} \cdot k_{LH} \cdot \frac{\left(1 + c_{LHp} \cdot P4^{\delta}\right)}{(1 + c_{LHe} \cdot E2)} - r_{LH} \cdot LH \tag{14}$$

$$\frac{d}{dt}RP_{FSH} = \frac{V_{FSH}}{1 + \left(\dfrac{InhA(t-d_{InhA})}{Ki_{FSHa}}\right) + \left(\dfrac{InhB(t-d_{InhB})}{Ki_{FSHb}}\right)} - k_{FSH} \cdot \frac{(1 + c_{FSHp} \cdot P4)}{(1 + c_{FSHe} \cdot E2^{\zeta})} \cdot RP_{FSH} \tag{15}$$

$$\frac{d}{dt}FSH = \frac{1}{v} \cdot k_{FSH} \cdot \frac{(1 + c_{FSHp} \cdot P4)}{(1 + c_{FSHe} \cdot E2^{\zeta})} \cdot RP_{FSH} - r_{FSH} \cdot FSH \tag{16}$$

Through changes in GnRH pulse frequency and amplitude, LH exhibits a biphasic response to E2 [23], so to account for this the model assumes that the effect of E2 on LH synthesis is different than the effect on LH release. E2 inhibits release (see the denominator of the second term of eq. (13)) but at high levels E2 promotes synthesis (see the numerator of the first term of (13)). On the other hand, P4 inhibits GnRH modulated LH synthesis

but promotes its release from the pituitary. The release term in (13) appears as a growth term in (14), where it is divided by blood volume v. The equations (15) and (16) for FSH are similar except the synthesis term has constant growth and inhibition due to InhA and InhB. Since hormone synthesis is a biochemical process more complicated than hormone release, we allow for discrete time-delays, d_E, d_P, d_T, d_{InhA} and d_{InhB}, in the synthesis terms.

2.6 Parameter Identification and Periodic Solution

Parameter estimation began with the best-fit parameters reported by Pasteur [34]. Nelder-Meade algorithm with least squares approximation optimized final parameters against data for normal mean serum levels for E2, P4, LH, FSH, InhA, and InhB as published by Welt *et al.* [49] and data for normal serum Total T levels as reported in Sinha-Hikim *et al.* [45]. Supplementation of the Welt data set was necessary as a single data set for all seven serum hormones was not available at the time of this publication. The original data reported by Sinha-Hikim *et al.* [45] included nine data points over 26 days. Therefore, linear extrapolation was used to generate 28 data points (see Figure 5) for optimal parameter estimation. For comparison purposes we converted the Sinha-Hikim data from nmol/L to ng/dL. This conversion takes the range of values from $(0.7, 1.6)$ to $(20, 47)$. The best-fit parameter set is detailed in Appendix A, Tables 1 through 4 .

The discrete time-delays present in the model (d_T, d_E, d_P, d_{InhA}, and d_{InhB}) necessitate the use of a delay differential equation solver *DDE23* by Shampine and Thompson available through MatLab 2010a [27] to numerically approximate a solution. Day 1 values from Welt *et al.* [49] served as initial conditions for LH and FSH equations. Numerical simulations with the best-fit parameter set exhibit an asymptotically stable periodic solution of period 29 days (Figure 6) consistent with reports of average cycle lengths between 26 and 32

days [12]. Once this stable periodic solution was identified, the remainder of the initial conditions were determined by the values from the last day of simulation. Rounded to four significant digits, our initial condition vector is detailed in Appendix A, Table 5.

3 Results

3.1 Numerical Simulations

Given the parameters listed in Tables 1 through 4, Figures (3)-(4) represent serum concentrations of LH, FSH, E2, P4, InhA, and InhB for 58 days as predicted by the model, with daily data for mean serum levels from Welt *et al.* [49] for comparison (the 28 data values reported in [49] are repeated here to obtain 58 data values). Two complete 29 day cycles are presented for each hormone to support the stability conclusion.

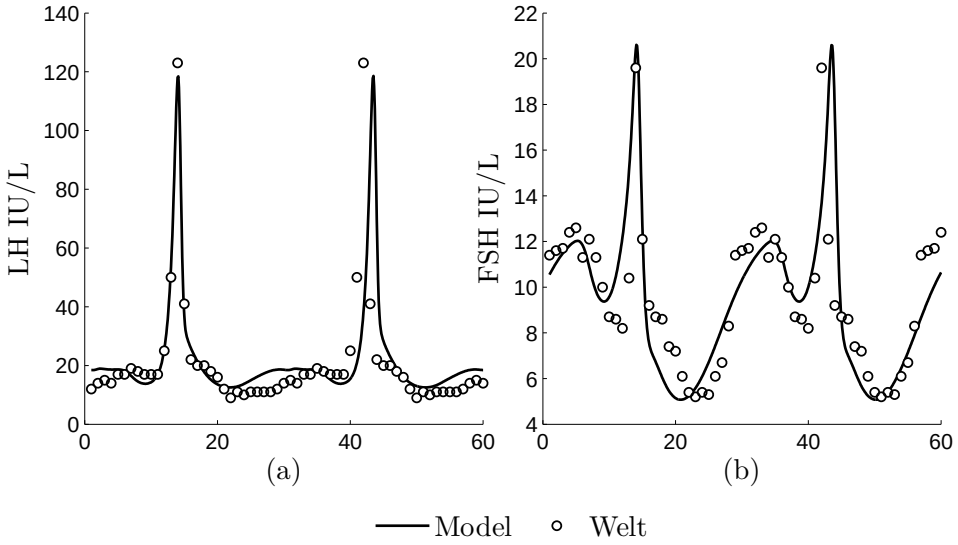

Figure 3: Two 29 day cycles for (a) LH data from Welt *et al.* (∘)and (b) FSH data from Welt *et al.* (∘) are presented with current model simulations (solid curves).

One can observe the qualitative similarities to clinical observations. Serum T concen-

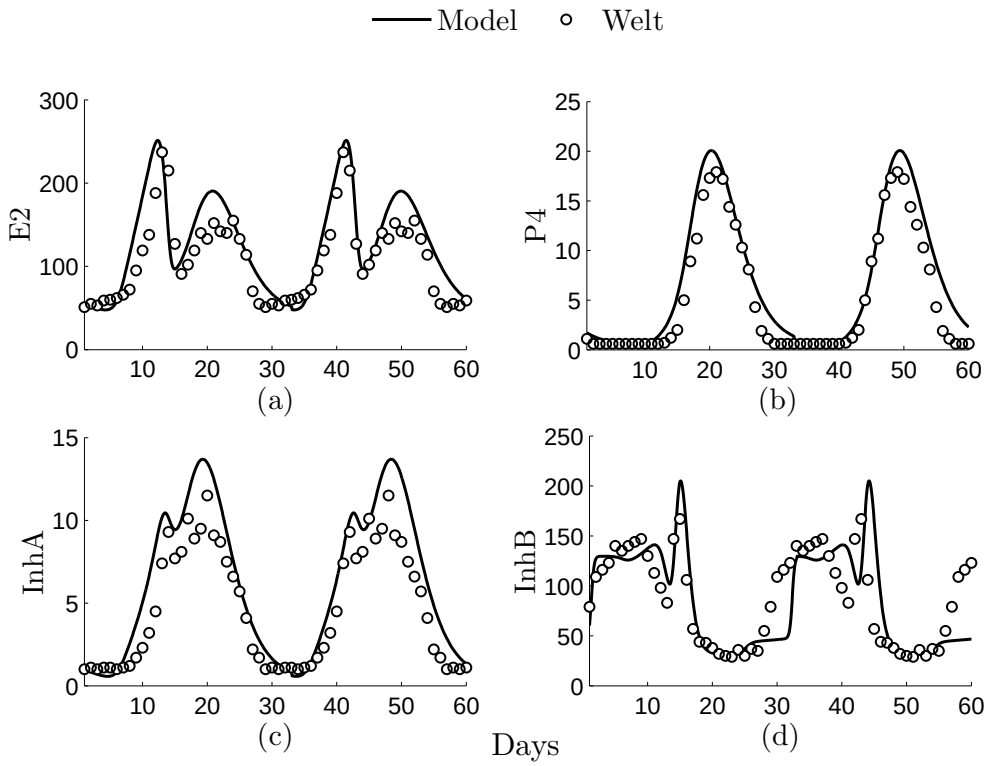

Figure 4: Two 29 day cycles for (a) E2 data from Welt *et al.* (∘) , (b) P4 data from Welt *et al.* (∘) , (c) InhA data from Welt *et al.* (∘), (d) InhB data from Welt *et al.* (∘) are presented with model simulations (solid curves).

trations for a 29 day simulation follow in Figure 5. Approximated T levels increase from a day 3 level of 30 ng/dL to a maximum level of 44 ng/dL on day 11 of the cycle. After ovulation, T slowly declines, plateauing from day 17 to 22 at approximately 34 ng/dL. At the end of the luteal phase, levels continue to decline before a slight rebound in circulating levels is observed during the luteal to follicular transition. Figure 5 presents data extracted from Sinha-Hikim *et al.* [45] against model predictions for comparison.

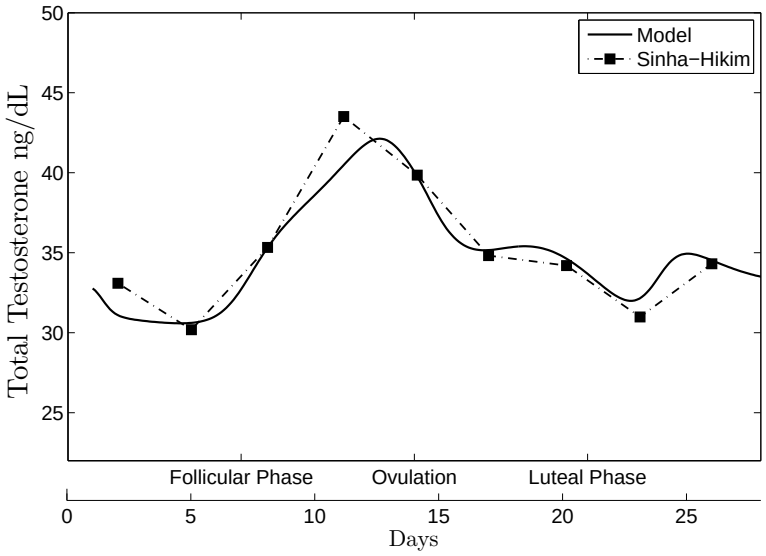

Figure 5: The nine T data points (■) from Sinha-Hikim *et al.* [45] are graphed with linear interpolation (– · –) and current model simulation (solid curve)

3.2 Modeling Predictions Regarding Stockpiling of Follicles

Irregularities in cycle length are commonly seen in patients with PCOS. As a common cause of infertility, PCOS affects up to 10% of reproductive age women and significantly correlates with increased risk of Type II diabetes and its associated morbidity [1, 3, 33]. Common phenotypes of PCOS also include elevated androgens and the appearance of polycystic ovaries on ultrasound [2], both significant components in the etiology of PCOS [15, 29, 40]. Histological studies of tissue samples taken from clinically diagnosed PCOS patients, recently reported by Maciel *et al.* [25] , suggests a "stockpiling" of preantral follicles when compared to controls. Their findings show a significantly ($P = .001$) increased number of follicles comprised of an oocyte and a single layer of cuboidal granulosa cells, i.e., primary follicles. It is hypothesized that the increase in primary follicle numbers is due to a longer growth pattern during this stage, represented by PrA1 in our model. We investigate m_2 as a possible model parameter to test this hypothesis. Because m_2 is measurement of mass transferred out of the primary stage, decreasing m_2 should delay primary follicle

maturation, permitting additional growth of primary follicles.

For comparison, we begin by presenting LH concentrations from the stable periodic solution that best fits data from Welt and Sinha-Hikim in Figure 6, i.e., the solution with parameters listed in Tables 1 through 4. This simulation is graphed for 7 months showing a stable solution having an average cycle length of approximately 29 days, consistent with reports from Baerwald *et al.* [4] and Gougeon *et al.* [12]. We assume ovulation coincides with the LH surge given a follicle of sufficient size is available for rupture. Hence, we present Figure 6 to depict 7 ovulations and the first 3 ovarian stages for comparison with Figures 7, 8 and 9, where the parameter m_2 has decreased. As the exact surge level of LH necessary to induce ovulation is unique to each woman, we identify (by thick horizontal lines in Figure 6) LH levels at 75% and 50% of the mean maximum LH level reported by Welt *et al.* [49] for possible threshold references. While the ovarian mass values for PrA1 through SmAn (Figure 6) are unitless, we note that the first preantral follicle mass peaks at approximately 20 units before transferring to the second androgen dependent preantral follicle mass. Follicular mass during this time is presented to demonstrate the interaction between the mass of developing follicles and ovulation assuming that surge levels of LH are indicative of the existence and timing of ovulation.

Figure 7 demonstrates the effect of reducing m_2 by approximately 50% of the best fit value in Table 3. Analysis of the resulting behavior, over 7 months, reveals an LH surge exceeding 150 IU/L followed by a surge approximately 20 IU/L lower. While each peak surge occurs monthly, the pattern of alternating surge levels takes over two months to repeat. Similarly the first preantral follicle mass begins to oscillate with a maximum mass of 30 units that results in lower mass transfer to the second preantral mass. In the normal case, our cycle length and the time for LH levels to return to the peak level of the previous cycle were the same. Reducing the transfer rate from PrA1 approximately

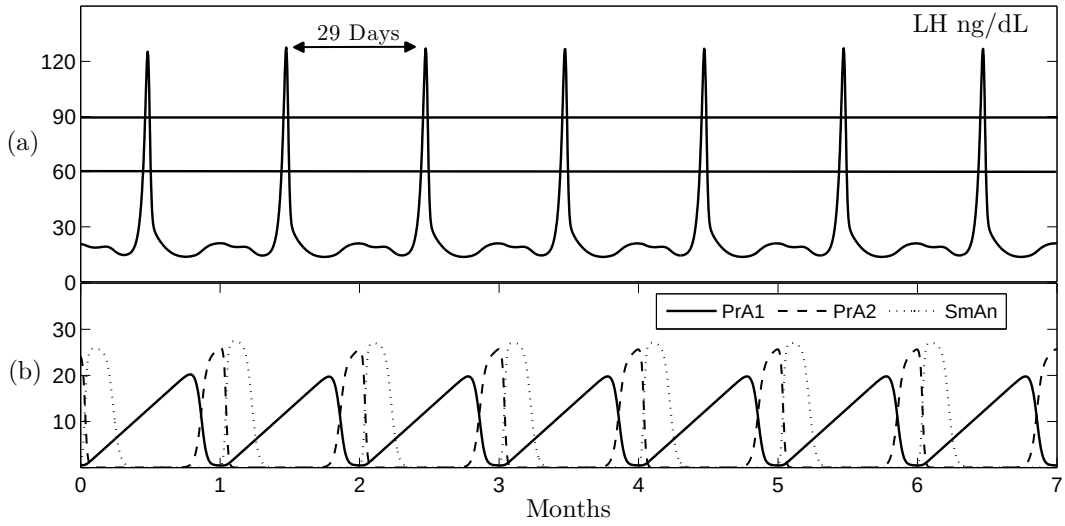

Figure 6: (a) Simulated serum LH IU/L over 7 months with reference lines for 75% and 50% of mean Welt surge levels (b) First 3 stages of follicular development, PrA1, PrA2, and SmAn

doubles the time between peaks of the same magnitude, a phenomenon know as a period-doubling event (the period of the solution to our model equations is now $\sim$ 64 days). Identification of this behavior is mathematically significant for systems of this size and complexity. Although period-doubling often occurs in systems of non-linear equations, it has rarely been demonstrated in a physiological model which predicts data in the literature. As demonstrated in Figure 8, reducing m_2 to 30% of the best-fit value in Table 3, results in LH surges of four distinct values. In this simulation the pattern of peak variation now repeats every 5.5 months with an average time between surges of approximately 40 days (another period-doubling has occurred). Examination of the resulting follicular mass reveals a distinct pattern of elevated PrA1, stockpiling of preantral follicles, that completes its transfer to subsequent stages over a period of approximately 80 days. This suggests correlation between preantral growth and irregular menstrual cycles consistent with the "stockpiling" hypothesis of Maciel *et al.* [25]. Mathematically this behavior indicates the existence of a period-doubling cascade of bifurcations as m_2 is decreased.

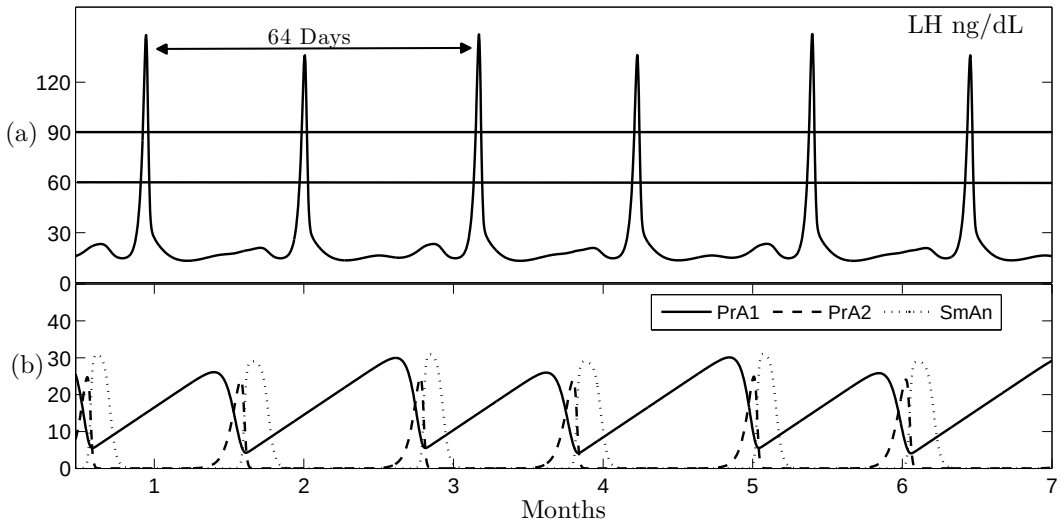

Figure 7: (a) Serum LH level results after a 50% reduction in parameter m_2 from best-fit value in Table 3 (b) Note the increase in PrA1 from Figure 6

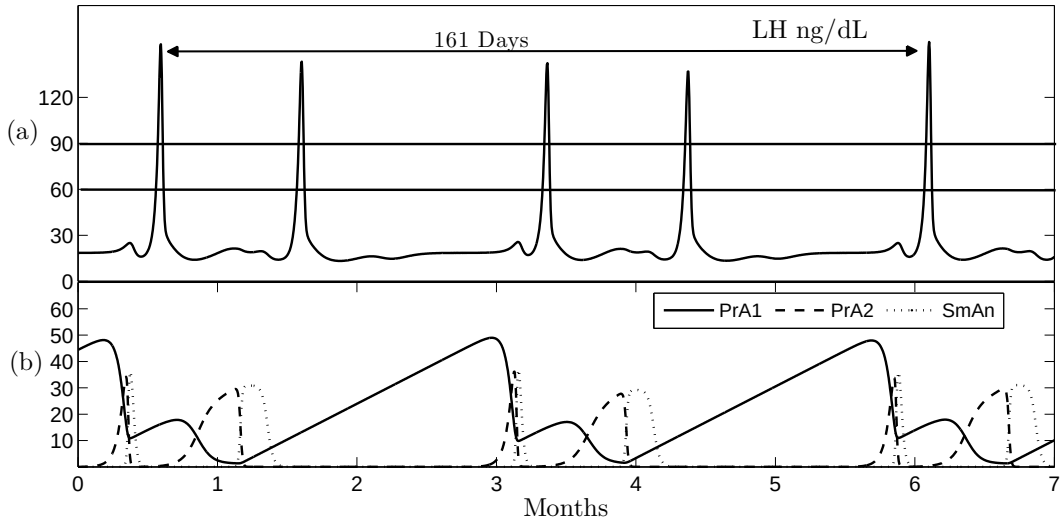

Figure 8: (a) Serum LH level results after a 70% reduction parameter m_2 best-fit value in Table 3 (b) First three stages of follicular development.

Complex dynamical systems with period-doubling cascades are often associated with chaotic behavior [41]. Investigating this phenomenon motivated numerical experiments

with additional decreases in m_2 to identify behavior consistent with chaotic attractors. Reducing m_2 by an additional 5% causes the disappearance of the stable 4-cycle shown in Figure 8 and the appearance of an apparent chaotic attractor as demonstrated in Figure 9. Also, a common characteristic of chaotic behavior, i.e., the existence of a stable 3-cycle, appears in a very narrow range of m_2 values near 26% of the value reported in Table 3. (Due to the lack of biological relevance of the 3-cycle solution, the results are not presented, merely noted.) If one assumes an LH threshold at 75% of the reported mean, as demonstrated by the top horizontal line in Figure 9, then the solution presented would ovulate approximately 5 times per year given the availability of a dominant follicle at the time of LH surge. Reducing the threshold assumption to 50% increases the frequency of ovulation to an average 8 cycles annually over the three year window presented. These frequencies are consistent with a clinical diagnosis of oligomenorrhea, infrequent menstruation with 4 to 8 menstrual cycles per year, a primary phenotype of PCOS. The appearance of low amplitude peaks that do not exceed threshold values observed in Figure 9 may be consistent with non-ovulatory LH surges discussed in Baerwald *et al.* 2012 [5].

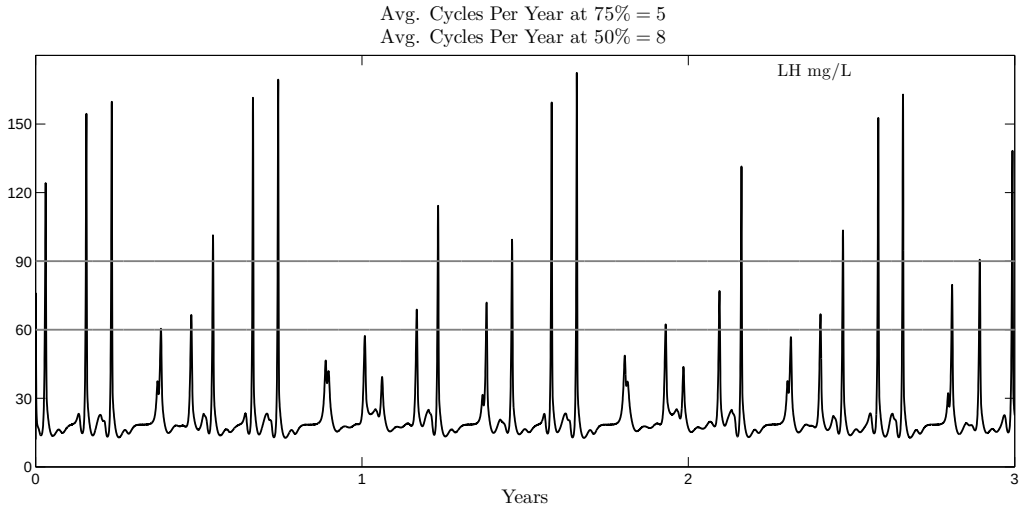

Figure 9: Chaotic serum LH levels observed over 3 years as m_2 is reduced to 25% of the best-fit value in Table 3. If ovulation occurs for an LH surge over 90 mg/L (75 % of the normal LH surge) then ~ 5 ovulations occur per year. If ovulation occurs for an LH surge over 60 mg/L then ~ 8 occur per year.

4 Summary and Discussion

This study presents a nonlinear mechanistic model for the endocrine regulation of the human menstrual cycle which consists of 16 delay differential equations and 5 auxiliary equations, with 71 parameters identified using data from the literature. Model simulations predict serum levels of LH, FSH, E2, P4, InhA, InhB and Testosterone consistent with biological data [45, 49]. The asymptotically stable periodic solution resulting from the best-fit parameter set (Tables 1 through 4) has a period of 29 days, consistent with current literature. Moreover, increases in qualitative accuracy are obtained through the use of mass action kinetic theory to describe preantral follicular through early antral follicular stage growth. We believe this is the first model of its type to be able to predict serum T levels in a mathematical context that allows analysis of bifurcations and stable solutions of various periods.

A benefit of this approach, is the identification of stable solutions that may resemble hormonal profiles consistent with some of the 16 PCOS phenotypes as defined in the Rotterdam consensus document [13]. While it is generally agreed that T plays an important role in PCOS, only 8 of the 16 PCOS phenotypes present with elevated androgens [13]. It is hypothesized that extended preantral follicular development could play an important role in explaining the appearance of polycystic ovaries [25], a significant criterion in normal patients. Our approach of reflecting intra-ovarian follicular growth regulation systemically allows researchers to investigate effects of preantral growth abnormalities on menstrual cycle behavior. In our investigation, observations from increasing preantral follicle growth duration support the hypothesis presented by Maciel *et al.* [25] that a "stockpiling" of immature follicles may be significant in the etiology of PCOS. Figures 6 through 9 reinforce this conclusion by demonstrating that the reduction of m_2 from its best-fit value in Table 3, which delays the transfer from preantral growth to androgen dependent growth, results in a visible "stockpiling" of preantral follicular mass (Figures 7 and 8) and in irregular cyclicity (Figure 9).

Furthermore, the identification of a period-doubling cascade of bifurcations leading to apparent chaotic behavior (Figure 9) may actually increase accuracy in representing clinical findings of women with PCOS and/or oligomenorrhea over previous models. A recent paper by Derry and Derry [8] presents a time series analysis of longitudinal menstrual cycle length data for 40 women over 20 to 40 years. They concluded that the human "menstrual cycle is the result of chaos in a nonlinear dynamical system" [8] with only 5 degrees of freedom. They further referenced specifically the model of Harris-Clark *et al.* [14] with the assertion that "any model producing only perfectly periodic menstrual cycles is, at best, incomplete" [8]. It is our belief that our current approach meets their criteria for a model of the human menstrual cycle that displays biologically relevant random behavior independent of external interference. It also shows that follicular dynamics cannot be abandoned in the

quest for accuracy, rather it is the interplay between intra-ovarian mass and endocrine regulation that explains this behavior.

We anticipate the emerging collaborations with clinical endocrinologists and experimentalists will soon provide essential data necessary to refine additional parameter sets that can simulate additional PCOS phenotypes. Preliminary investigations include manipulating serum T levels, through altering t_1, as a reflection of excess adrenal androgen production, and t_3, as a reflection of increased insulin dependent theca cell T synthesis. These studies support the consideration of androgenic feedback on LH synthesis and encourage further examination of its effect on FSH synthesis. We believe these investigations will lend further understanding to PCOS phenotypes and adrenal disorders that present with elevated androgens.

The basic assumption that the hypothalamus-pituitary-ovarian axis is in itself a closed autonomous dynamical system presenting stable yet possibly chaotic behavior has led us to the development and presentation of our current model for endocrine regulation of female reproduction. Numerical approximations of stable solutions can be quickly computed as compactness was a major consideration in model development. These attributes make it a prime candidate for *in-silico* investigations of cycle regularity. We have shown that modeling biological mechanisms, while considering clinical challenges and computational costs can lead to mathematically rich dynamics that present new model-derived insights that may guide future development of innovative individualized therapeutic interventions for women with PCOS.

Appendices

A Parameters and Inital Conditions

Table 1: LH Subsystem Parameters

Parameter	Value	Unit
$v_{0_{LH}}$	33.3	μ/day
$v_{1_{LH}}$	160.75	μ/day
Ki_{LH}	13.6	$L/nmol$
Km_{LH}	47.33	ng/L
k_{LH}	19.99	$1/day$
c_{LH_P}	.98	$L/nmol$
c_{LH_E}	.9	L/ng
d_P	1	$days$
d_T	0	$days$
d_E	0	$days$
κ	.92	$dimensionless$
δ	2	$dimensionless$
a	6.07	$dimensionless$
r_{LH}	14	$1/\text{day}$
v	2.5	$liters$

Table 2: FSH Subsystem Parameters

Parameter	Value	Unit
v_{FSH}	283.99	μ/day
Ki_{FSH_a}	6.38	μ/day
Ki_{FSH_b}	3000	L/nmol
k_{FSH}	3.41	$1/\text{day}$
c_{FSH_p}	1.26	L/nmol
c_{FSH_e}	0.16	L/ng
ζ	.84	$dimensionless$
d_{InhA}	1	$days$
d_{InhB}	1	$days$
r_{FSH}	8.21	$1/\text{day}$

Table 3: Ovarian Subsystem Parameters

Parameter	Value	Unit	Parameter	Value	Unit
α	0.7100	dimensionless	k_1	0.7089	$1/\text{day}$
β	0.6928	dimensionless	k_2	0.8712	$1/\text{day}$
γ	0.0002	dimensionless	k_3	1.038	$1/\text{day}$
ξ	0.952	dimensionless	k_4	1.052	$1/\text{day}$
b	0.0189	L/day	m_1	0.9274	$1/\text{day}$
c_1	0.0871	$\text{L}/\mu\text{g}$	m_2	1.338×10^{-3}	$1/\text{day}$
c_2	0.1251	$1/\text{day}$	η	1.162	$1/\text{day}$
c_3	0.0533	$1/\text{day}$	m_3	0.15	$1/\text{day}$
c_4	0.0371	$1/\text{day}$	Km_{FSH}	7.533	$1/\text{day}$
c_5	0.4813	$1/\text{day}$	ν	8	$1/\text{day}$
d_1	0.7053	$1/\text{day}$	ϱ	0.451	$1/\text{day}$
d_2	0.6488	$1/\text{day}$			

Table 4: Auxiliary Equations Parameter Set

Parameter	Value	Unit	Parameter	Value	Unit
Parameter	Value	Unit	Parameter	Value	Unit
e_0	38.25	$^{ng}/_{L}$	j_4	3.411	$^{1}/_{L}$
e_1	2.3	$^{1}/_{kL}$	j_5	3	$^{1}/_{L}$
e_2	2.724	$^{1}/_{kL}$	j_6	0.0012	$^{1}/_{L}$
h_0	0.0525	$^{U}/_{L}$	t_1	21.92	$^{ng}/_{dL}$
h_1	0.0251	$^{nmol/L}/_{\mu g}$	t_2	0.3721	$^{1}/_{dL}$
h_2	0.06315	$^{U}/_{L}$	t_3	0.2961	$^{1}/_{dL}$
h_3	0.1584	$^{U}/_{L}$	t_4	0.4538	$^{1}/_{dL}$
p_1	0.2548	$^{nmol/L}/_{\mu g}$	t_5	0.0411	$^{1}/_{dL}$
p_2	0.1276	$^{nmol/L}/_{\mu g}$	t_6	0.7029	$^{1}/_{dL}$
j_1	27.21	$^{pg}/_{L}$	t_7	0.0459	$^{1}/_{dL}$
j_2	1.885	$^{1}/_{L}$	t_8	0.1998	$^{1}/_{dL}$
j_3	3.738	$^{1}/_{L}$			

Table 5: Initial Conditions

State Variable	Initial Condition
RP_{LH}	1071
LH	12.0
RP_{FSH}	155.6
FSH	11.40
PrA1	.6112
PrA2	15.11
SmAn	12.36
RcF	.1511
DmF	1.337
OvF	1.168
CL1	1.003
CL2	1.865
Lut1	3.265
Lut2	4.071
Lut3	6.055
Lut4	9.029

References

[1] Alvarez-Blasco, F., Botella-Carretero, J.I., San Millán, J.L., Escobar-Morreale, H.F.: Prevalence and characteristics of the polycystic ovary syndrome in overweight and obese women. Archives of Internal Medicine **166**(19), 2081–6 (2006). DOI 10.1001/archinte.166.19.2081

[2] Azziz, R., Carmina, E., Dewailly, D., Diamanti-Kandarakis, E., Escobar-Morreale, H.F., Futterweit, W., Janssen, O.E., Legro, R.S., Norman, R.J., Taylor, A.E., Witchel, S.F.: The Androgen Excess and PCOS Society criteria for the polycystic ovary syndrome: the complete task force report. Fertility and Sterility **91**(2), 456–488 (2009)

[3] Azziz, R., Woods, K.S., Reyna, R., Key, T.J., Knochenhauer, E.S., Yildiz, B.O.: The prevalence and features of the polycystic ovary syndrome in an unselected population. The Journal of Clinical Endocrinology & Metabolism **89**(6), 2745–9 (2004). DOI 10.1210/jc.2003-032046

[4] Baerwald, A.R., Adams, G.P., Pierson, R.a.: A new model for ovarian follicular development during the human menstrual cycle. Fertility and Sterility **80**(1), 116–122 (2003). DOI 10.1016/S0015-0282(03)00544-2

[5] Baerwald, A.R., Adams, G.P., Pierson, R.A.: Ovarian antral folliculogenesis during the human menstrual cycle: a review. Human Reproduction Update **18**(1), 73–91 (2012). DOI 10.1093/humupd/dmr039

[6] Baird, R.T., Horton, R., Longcope, C., Tait, J.F.: Steroid dynamics under steady-state conditions. Recent Progress in Hormone Research **25**, 611–664 (1969)

[7] Bogumil, R.J., Ferin, M., Rootenberg, J., Speroff, L., Vande Wiele, R.L.: Mathematical studies of the human menstrual cycle. I. Formulation of a mathematical model. The Journal of Clinical Endocrinology & Metabolism **35**(1), 126–43 (1972)

[8] Derry, G., Derry, P.: Characterization of chaotic dynamics in the human menstrual cycle. Nonlinear Biomedical Physics **4**(1), 5 (2010). DOI 10.1186/1753-4631-4-5

[9] Fauser, B.C., Van Heusden, A.M.: Manipulation of human ovarian function: physiological concepts and clinical consequences. Endocrine Review **18(1)**(1), 71–106 (1997)

[10] Fihri, A.F., Hajji, K.H., Lakhdissi, H.: Histological exploration of follicular population of the Moroccan bovine (Oulmes-Zaers) breed. African Journal of Biotechnology **3**(May), 294–298 (2004)

[11] Franks, S., Stark, J., Hardy, K.: Follicle Dynamics and anovulation in polycystic ovary syndrome. Human Reproduction Update **14**(4), 1–12 (2008)

[12] Gougeon, A.: Dynamics of follicular growth in the human: a model from preliminary results. Human Reproduction (Oxford, England) **1**(2), 81–7 (1986)

[13] Consensus workshop group, T.R.E.S.P.: 2004 Rotterdam 1: revised 2003 consensus on diagnostic criteria and long-term health risks related to polycystic ovary syndrome (PCOS). Human Reproduction **19**(1), 41–47 (2004)

[14] Harris-Clark, L., Schlosser, P.M., Selgrade, J.F.: Multiple stable periodic solutions in a model for hormonal control of the menstrual cycle. Bulletin of Mathematical Biology **65**(1), 157–73 (2003). DOI 10.1006/bulm.2002.0326

[15] Hillier, S.G., Ross, G.T.: Effects of exogenous testosterone on ovarian weight, follicular morphology and intraovarian progesterone concentration in estrogen-primed hypophysectomized immature female rats. Biology of Reproduction **20**, 261–268 (1979)

[16] Hotchkiss, J., Knobil, E.: The menstrual cycle and its neuroendocrine control. In: E. Knobil, J. Neill (eds.) The Physiology of Reproduction, Second Edition, pp. 711–750. Raven Press, New York (1994)

[17] J.F. Selgrade, P.M. Schlosser: A model for the production of ovarian hormones during the menstrual cycle. Fields Institute Communications **21**, 429–446 (1999)

[18] Jonard, S., Dewailly, D.: The follicular excess in polycystic ovaries, due to intra-ovarian hyperandrogenism, may be the main culprit for the follicular arrest. Human Reproduction Update **10**(2), 107–17 (2004). DOI 10.1093/humupd/dmh010

[19] Karch, F., Dierschke, D., Weick, R., Yamaji, T., Hotchkiss, J., Knobil, E.: Positive and negative feedback control by estrogen of luteinizing hormone secretion in the rhesus monkey. Endocrinology **92**(3), 799–804 (1973). DOI 10.1210/endo-92-3-799

[20] Keener, J., Sneyd, J.: Mathematical Physiology I: Cellular Physiology, second edn. Springer-Verlag, New York (2009)

[21] Kuo, S.W., Ke, F.C., Chang, G.D., Lee, M.T., Hwang, J.J.: Potential role of follicle-stimulating hormone (FSH) and transforming growth factor (TGFβ1) in the regulation of ovarian angiogenesis. Journal of Cellular Physiology **226**(6), 1608–19 (2011). DOI 10.1002/jcp.22491

[22] Lass, A.: The role of ovarian volume in reproductive medicine. Human Reproduction Update **5**(3), 256–266 (1999). DOI 10.1093/humupd/5.3.256

[23] Liu JH, Y.S.S.: Induction of midcycle surge by ovarian steriods in women: A critical evaluation. Journal of Clinical Endocrinology **57(4)**, 797–802 (1983)

[24] Lucy, M.C.: Growth hormone regulation of follicular growth. Reproduction, Fertility, and Development **24**(1), 19–28 (2011). DOI 10.1071/RD11903

[25] Maciel, G.A.R., Baracat, E.C., Benda, J.A., Markham, S.M., Hensinger, K., Chang, R.J., Erickson, G.F.: Stockpiling of transitional and classic primary follicles in ovaries of women with polycystic ovary syndrome. The Journal of Clinical Endocrinology & Metabolism **89**(11), 5321–7 (2004). DOI 10.1210/jc.2004-0643

[26] Margolskee, A., Selgrade, J.F.: Dynamics and bifurcation of a model for hormonal control of the menstrual cycle with inhibin delay. Mathematical Biosciences **234**(2), 95–107 (2011). DOI 10.1016/j.mbs.2011.09.001

[27] Matlab: version 7.14 (R2012a). The MathWorks Inc., Natick, Massachusetts (2012)

[28] McLachlan, R., Cohen, N., Dahl, K., Bremner, W., Soules, M.: Serum inhibin levels during the periovulatory interval in normal women: Relationships with sex steroid and gonadotrophin levels. Clinical Endocrinology **1**(32), 39–48 (1990)

[29] Medina, F., Nestler, J.: Insulin Stimulates Testosterone Biosynthesis by Human Theca Cells from Women with Polycystic Ovary Syndrome by Activating its own receptor and using inositoglycan mediators as the signal transduction system. Journal of Clinical Endocrinology & Metabolism **83(6)**, 2001–2005 (1998)

[30] Nussey, S.S., Whitehead, S.A.: Endocrinology : An Integrated Approach. Taylor & Francis, London (2001)

[31] Odell, W.: The Reproductive System in Women. In: L. DeGroot (ed.) Endocrinology, pp. 1393–1400. Grune & Stratton, New York (1979)

[32] Orisaka, M., Tajima, K., Tsang, B.K., Kotsuji, F.: Oocyte-granulosa-theca cell interactions during preantral follicular development. Journal of Ovarian Research **2**(1), 9 (2009). DOI 10.1186/1757-2215-2-9

[33] Panidis, D., Macut, D., Farmakiotis, D., Rousso, D., Kourtis, A., Katsikis, I., Spanos, N., Petakov, M., Bjekic, J., Damjanovic, S.: Indices of insulin sensitivity, beta cell function and serum proinsulin levels in the polycystic ovary syndrome. European Journal of Obstetrics, Gynecology, and Reproductive Biology **127**(1), 99–105 (2006). DOI 10.1016/j.ejogrb.2005.12.016

[34] Pasteur, R.: A multiple-inhibin model for the human menstrual cycle. Ph.D. thesis, North Carolina State University (2008)

[35] Pasteur, R., Selgrade, J.: A deterministic, mathematical model for hormonal control of the menstrual cycle. In: W. Dubitzky, J. Southgate, H. Fu\ss (eds.) Understanding the Dynamics of Biological Systems: Lessons Learned from Integrative Systems Biology, pp. 38–58. Singer, London (2011)

[36] Pielecka, J., Quaynor, S.D., Moenter, S.M.: Androgens increase gonadotropin-releasing hormone neuron firing activity in females and interfere with progesterone negative feedback. Endocrinology **147**(3), 1474–9 (2006). DOI 10.1210/en.2005-1029

[37] Reddy, P., Zheng, W., Liu, K.: Mechanisms maintaining the dormancy and survival of mammalian primordial follicles. Trends in Endocrinology and Metabolism **21**(2), 96–103 (2010). DOI 10.1016/j.tem.2009.10.001

[38] Reinecke, I., Deuflhard, P.: A complex mathematical model of the human menstrual cycle. Journal of Theoretical Biology **247**(2), 303–30 (2007). DOI 10.1016/j.jtbi.2007.03.011

[39] Rice, S., Ojha, K., Whitehead, S., Mason, H.: Stage-specific expression of androgen receptor, follicle-stimulating hormone receptor, and anti-Müllerian hormone type II receptor in single, isolated, human preantral follicles: relevance to polycystic ovaries.

Journal of Clinical Endocrinology & Metabolism **92**(3), 1034–1040 (2007). DOI 10.1210/jc.2006-1697

[40] Ropelato, M.G., García Rudaz, M.C., Escobar, M.E., Bengolea, S.V., Calcagno, M.L., Veldhuis, J.D., Barontini, M.: Acute effects of testosterone infusion on the serum luteinizing hormone profile in eumenorrheic and polycystic ovary syndrome adolescents. Journal of Clinical Endocrinology & Metabolism **94**(9), 3602–3610 (2009). DOI 10.1210/jc.2009-0402

[41] Sander, E., Yorke, J.: Connecting period-doubling cascades to chaos. International Journal of Bifurcation and Chaos **22**, 1–29 (2012)

[42] Schlosser, P., Selgrade, J.: A model of gonadotropin regulation during the menstrual cycle in women: Qualitative features. Environ. Health Perspect. **108**(5), 873–881 (2000)

[43] Selgrade, J.F.: Bifurcation analysis of a model for hormonal regulation of the menstrual cycle. Mathematical Biosciences **225**(2), 108–14 (2010). DOI 10.1016/j.mbs.2010.02.004

[44] Selgrade, J.F., Harris, L.A., Pasteur, R.D.: A model for hormonal control of the menstrual cycle: Structural consistency but sensitivity with regard to data. Journal of Theoretical Biology **260**(4), 572–580 (2009). DOI 10.1016/j.jtbi.2009.06.017

[45] Sinha-Hikim, I., Arver, S., Beall, G., Shen, R., Guerrero, M., Sattler, F., Shikuma, C., Nelson, J.C., Landgren, B.M., Mazer, N.a., Bhasin, S.: The use of a sensitive equilibrium dialysis method for the measurement of free testosterone levels in healthy, cycling women and in human immunodeficiency virus-infected women. The Journal of Clinical Endocrinology & Metabolism **83**(4), 1312–8 (1998)

[46] Skinner, M.K.: Regulation of primordial follicle assembly and development. Human Reproduction Update **11(5)**, 461–471 (2005)

[47] Taylor, A., Mccourt, B., Martin, K.A., Anderson, E.J., Adams, J.M., Schoenfeld, D., Hall, J.E.: Determinants of abnormal gonadotropin secretion in clinically defined women with polycystic ovary syndrome. Journal of Clinical Endocrinology & Metabolism **82**(7), 2248–2256 (1997)

[48] Vetharaniam, I., Peterson, a.J., McNatty, K.P., Soboleva, T.K.: Modelling female reproductive function in farmed animals. Animal Reproduction Science **122**(3-4), 164–73 (2010). DOI 10.1016/j.anireprosci.2010.08.015

[49] Welt, C.K., McNicholl, D.J., Taylor, A.E., Hall, J.E.: Female reproductive aging is marked by decreased secretion of dimeric inhibin. The Journal of Clinical Endocrinology & Metabolism **84**(1), 105–11 (1999)

[50] Yasin, M., Dalkin, A., Haisenleder, D., Marshall, J.: Testosterone is required for gonadotropin-releasing hormone stimulation of luteinizing hormone-beta messenger ribonucleic acid expression in female rats. Endocrinology **137**(4) (1996)

[51] Yen, S.S.: The human menstrual cycle: Neuroendocrine regulation. In: S.S.C. Yen, R.B. Jaffe, R.L. Barbieri (eds.) Reproductive Endocrinology. Physiology, Pathophysiology and Clinical Management., 4th edn., pp. 191–217. W.B. Sauders Co., Philadelphia (1999)

[52] Zeleznik, A.J.: The physiology of follicle selection. Reproductive Biology and Endocrinology **2**, 31 (2004). DOI 10.1186/1477-7827-2-31